Eur. Phys. J. B (2013) 86: 13
DOI: 10.1140/epjb/e2012-30292-x

THE EUROPEAN PHYSICAL JOURNAL B

Regular Article

Risks of an epidemic in a two-layered railway-local area traveling network

Zhongyuan Ruan[1], Pakming Hui[2], Haiqing Lin[2], and Zonghua Liu[1,a]

[1] Department of Physics, East China Normal University, Shanghai 200062, P.R. China
[2] Department of Physics, The Chinese University of Hong Kong, Shatin, New Territories, Hong Kong

Received 5 April 2012 / Received in final form 13 October 2012
Published online 21 January 2013 –

Abstract. In view of the huge investments into the construction of high speed rails systems in USA, Japan, and China, we present a two-layer traveling network model to study the risks that the railway network poses in case of an epidemic outbreak. The model consists of two layers with one layer representing the railway network and the other representing the local-area transportation subnetworks. To reveal the underlying mechanism, we also study a simplified model that focuses on how a major railway affects an epidemic. We assume that the individuals, when they travel, take on the shortest path to the destination and become non-travelers upon arrival. When an infection process co-evolves with the traveling dynamics, the railway serves to gather a crowd, transmit the disease, and spread infected agents to local area subnetworks. The railway leads to a faster initial increase in infected agents and a higher steady state infection, and thus poses risks; and frequent traveling leads to a more severe infection. These features revealed in simulations are in agreement with analytic results of a simplified version of the model.

1 Introduction

Countries such as the USA, Japan, and China are investing heavily on high speed rails [1] and other modern transportation systems like highways, subways and airports. They are essential for sustaining economic growth, but they also enhance the risk of a pandemic, as evidenced by the spread of SARS (severe acute respiratory syndrome), avian influenza and H1N1 swine influenza in the past decade. A highly desirable goal is to mitigate an epidemic while keeping the convenience of massive and rapid transportation. An important step towards this goal is to understand how modern transportation systems such as high speed trains could affect the dynamics of an epidemic and how possibly one could lower the risk.

Recent progress on epidemic spreading in complex networks guided us to focus on epidemics in multi-layered networks. Prior to the observation of the small-world (SW) and scale-free (SF) properties in many real-world networks, studies on epidemics were mainly focused on random or Erdos-Renyi (ER) networks in which every pair of nodes in a system has a certain probability to be connected, and fully mixed populations [2]. A main result is that there exists an epidemic threshold and an outbreak occurs only when the contagious rate is higher than the threshold. The discovery of SW and SF properties has led to much work on the effects of network topology on epidemics as related to the epidemic threshold [3–10], epidemics in SW networks [11,12], SF networks [13–18], community networks [19,20], networks with mobile agents [21–30], and immunization [31–36]. For studies on epidemics in a static network in which each node represents an immobile agent, it was found that a finite epidemic threshold does not exist in SF networks in the thermodynamic limit, indicating that a tiny initial infection can eventually spread [4–8,10]. The result is important in that it sheds light on the alarming risk of SARS, avian influenza, H1N1 swine influenza and other diseases. There are also studies on systems of multiple agents on a node with infectious process occurring only among agents staying on the same node, coupled with a diffusion of the agents among the nodes forming a modified version of reaction-diffusion processes [28,29]. More recently, there are studies on how human dynamics would affect an epidemic. These include studies on adaptive rewiring of connections among agents so as to avoid infections [37], agents traveling towards a destination instead of along a diffusive path and the effects of continual re-grouping [25,30,38]. The pattern of how a virus spreads among mobile phones [26] was also studied. These studies are representative of the trend of moving progressively closer to real-life situations.

Despite the progress, much remains to be done as real-world functional networks almost always involve the interconnection between two or more networks. An approach is to study systems consisting of multi-layered networks [39–43]. For example, traffic networks constructed based on flights, trains, and coaches are typical multi-layered networks. The epidemic spreading on

[a] e-mail: zhliu@phy.ecnu.edu.cn

airport networks has been well studied [28,44–46] and an interesting work focused on the multiscale mobility network consisting of short-scale commuting flows and long-range airline traffic [47]. Although these works have made a big progress in epidemic spreading, they still suffer from two unrealistic aspects. One concerns the assumption that agents are continually diffusing from one node to another. In reality, people travel to a desired destination and stop for a while before taking the next journey. Another assumption is that an airport and the local area that it serves are collectively represented by a node at which the agents interact in a well-mixed fashion. However, the local-area transportation network that brings people to and from the airport is quite different from the routes that fly people from one place to another. Thus, considering the movement of agents without distinguishing the local-area supporting network would be too simplistic for studying epidemics in the presence of travelers. The problem, instead, is that of an epidemic in a double-layered network. In the present work, we study an infection process in two-layer traveling network models. In view of the plans of building high speed trains in US, Japan and China, the model will be introduced within the context of major railways with stations supported by local-area subnetworks, and agents travel from one place within a subnetwork to another via the railway when an infection process co-evolves. In the USA, for example, the plan is to construct high speed rails with trains running at 220 mph supported by local-area networks running at 110 mph [1]. Our model incorporates the novel features that (i) people travel with an intended destination and their traveling paths connect the nodes in different local subnetworks in a shortest path; (ii) the railway serves to gather travelers and transmit infected individuals between different local subnetworks; and (iii) infections take place both on the railway and inside the local subnetworks. Numerical simulations show that both the single railway and the railway network accelerate the spreading of disease significantly, when compared with that in a corresponding ER network. Frequent traveling, as always required in modern city life, leads to a higher infection level and is thus risky. Raising the speed, as currently planned in many countries, would reduce infections. A qualitative understanding of the result is presented via an analysis of a simplified version of our model.

This paper is organized as follows. In Section 2, we introduce a two-layered railway-local area traveling network model. In Section 3, we simplify the model to one that consists only of a single major railway serving the local areas to address how a railway accelerates spread of an epidemic. In Section 4, we present a theoretical framework to explain the results of the simplified railway-local area traveling network. Results are summarized in Section 5.

2 Two-layer railway-local area traveling network model

We first study epidemics in a two-layered network model where one layer is a railway network and the other is a ground transport network, with connections between them. The layer consisting of the railway network is, in general, composed of multiple major railways that intersect at big cities. Considering the facts that there is only one railway station in a city in general and each city has its local-area transport network, we assume that each node of the railway network is accompanied with and connected to a local-area subnetwork. For simplicity, both the railway network and each local-area subnetwork are taken to be ER random networks. Figure 1 shows the two-layered railway-local area traveling network schematically. For clarity, the railway network is displaced vertically from the local area subnetworks, illustrating the two-layered structure. Traveling within an area invokes only the local-area subnetwork. In making a journey from one place to another, a traveler typically takes a path consisting of three parts: the traveler will go to the railway station via the local area subnetwork, use the railway network, and then another local area subnetwork to arrive at the destination. For each part of the journey, the shortest path is taken.

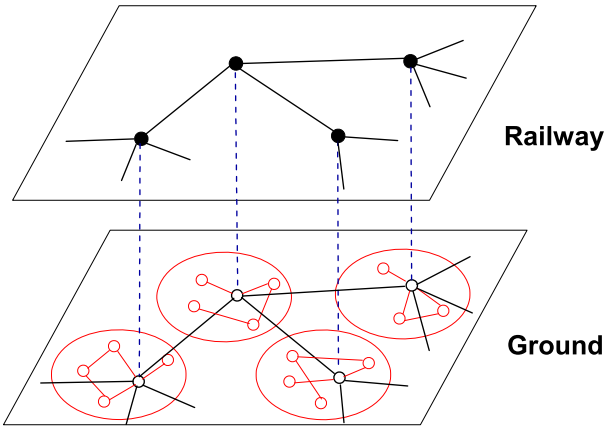

Fig. 1. (Color online) Schematic diagram of the two-layered railway-local area traveling network. The big circles outline the local-area subnetworks. The open circles represent local towns and the solid dots represent the railway stations serving different local areas. For clarity, the railway network is displaced vertically from the local area subnetworks.

More specifically, the model can be constructed as follows. Let $m = 50$ be the total number of nodes in the railway network and thus the number of local area subnetworks. This value of m is reasonable in that there are, for example, 48 major railway stations in China [48]. For each subnetwork i ($i = 1, \ldots, m$), it is constructed as an ER random network consisting of $M_i = 100$ nodes (towns) and the probability q of having a connection between any two nodes is $q = 0.1$, resulting in a mean degree of $\langle k \rangle = 10$. Therefore, the whole network has $M = 5000$ nodes. For each subnetwork, the node with the highest degree is chosen to be the railway station (black dots in Fig. 1) serving the local area. To construct the railway network, the $m = 50$ railway stations are also connected as an ER network with an average degree $\langle k \rangle = 10$.

To study infection in the two-layer network, we introduce people into the system. A total of $N = 5 \times 10^4$ persons, i.e. on average, $N/M = 10$ persons per node are introduced. Initially, N_i of them are distributed into the ith subnetwork, and they randomly occupy the nodes, but leaving the railway station empty. Each person is in one of two states: traveling or non-traveling. We assume that a non-traveling person has a probability p to turn into a traveling person at each time step, thus a person will stay in a place for an average of $1/p$ time steps before starting another journey. The initial condition implies that there are pN_i travelers and $(1-p)N_i$ non-travelers in the ith subnetwork.

People tend to take the shortest path towards their destination when they travel [30]. This is similar to the routing strategy for sending messages in the Internet [49]. This process is highly directional, and completely different from the non-directional random diffusion of particles on a network in which every neighboring node has a finite probability of receiving a particle. When a person turns into a traveler at a node i, he picks a node j randomly in the whole network as his destination. A railway station cannot be chosen as journey destination, as it serves only as a stop to get off for destinations in its local area. To model human travelers, every traveler takes on the shortest path. For nodes i and j belonging to different local areas, a traveler gets to the railway station via the shortest path in his local subnetwork, takes the railway to the railway station that node j belonging to, and then follows the shortest path to travel to the destination via the local-area subnetwork. The traveler moves one node per time step on the shortest path. Upon arrival at the node j, a traveler turns into a non-traveler and stays there, until his next journey begins. Therefore, there are both travelers and non-travelers on the nodes in the subnetworks, and there are only travelers in the railway stations.

To study how the railway network influences the epidemic spreading, we will study the susceptible-infected-susceptible (SIS) model of an epidemic, where S and I represent the susceptible and infected individuals. The SIS model is for diseases that cannot be immunized, and an infected person would recover and become susceptible again, as in tuberculosis and gonorrhea [4,7,8,15,19]. Following reference [28], infections take place only among persons located in the same node. Every susceptible may be infected by each of the infected persons at the same node, with each infection occurring at a probability β. Therefore, a susceptible at the node i will become infected with the probability $1-(1-\beta)^{n_{i,I}}$, where $n_{i,I}$ is the number of infected persons at the node i [28]. As many persons are allowed to be in a node, it is analogous to a bosonic reaction-diffusive process in networks [22,28–30], but now generalized to directed movements along the shortest paths.

An infection process is initialized by having 1% of the people randomly infected. The probability for a non-traveler to start a journey is $p = 0.05$, unless specified otherwise. The recovery probability is $\mu = 0.1$. A measurement of the extent of an epidemic is the density of infected persons in the system defined by $\rho_I = \sum_{i=1}^{M} n_{i,I}/N$.

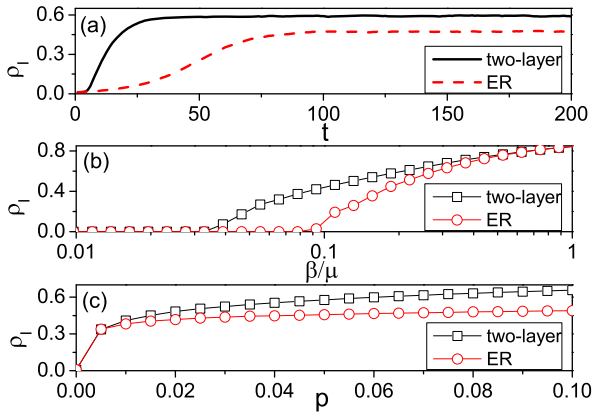

Fig. 2. (Color online) Results for SIS model. (a) ρ_I as a function of time t for $p = 0.05$, $\mu = 0.1$ and $\beta = 0.02$, for the two-layer railway-local area traveling network (solid line) and a corresponding ER random network (dashed line) with the same number of nodes and mean degree. (b) The steady-state value of ρ_I as a function of β/μ, for $p = 0.05$ and $\mu = 0.1$, in the two-layer network (squares) and the corresponding ER network (circles). (c) The effects of more frequent travelers, as represented by a higher traveling probability p. ρ_I (squares) as a function of p, for $\beta = 0.02$ and $\mu = 0.1$. Results are compared with that in the corresponding ER network (circles).

Figure 2a shows how ρ_I varies with time for the infection probability $\beta = 0.02$ (solid line) in the SIS model. The results show a rapid increase at short time followed by reaching a steady-state value. It should be noted that the choice of values for β and μ is taken from those in connection to the spread of H1N1 [50].

To demonstrate the effects a two-layered railway-local-area network, it is illustrative to compare results with a reference single-layer ER random network that has the same number of nodes $M = 5000$ and the same average degree $\langle k \rangle = 10$ as in the two-layered railway-local-area network. Simulations on this reference network show a slower increase in ρ_I at short time (see dashed line in Fig. 2a) and a smaller steady-state value. Thus, the railway network makes the epidemic more severe. Figure 2b shows the results of the steady-state ρ_I as a function of β/μ for both the two-layered railway-local-area and reference ER networks. The key feature is that a finite ρ_I results for a smaller value of β/μ in the presence of a railway network, indicating that the presence of the railway network enhances the spread.

Modern societies are characterized by frequent traveling, for reasons including a farther distance between home and workplace, traveling for business and for pleasure. There are periodic high traveling seasons, with an extreme example given by the over 0.3 billion long-distance travelers in China during the lunar new year period and most of them take a combination of railway and local area transportation. These situations correspond to a higher value of p in our models. Figure 2c shows how the steady state value of ρ_I varies with p in the SIS model with $\beta = 0.02$ and $\mu = 0.1$, for both the two-layer railway-local area travel network (squares) and the corresponding ER

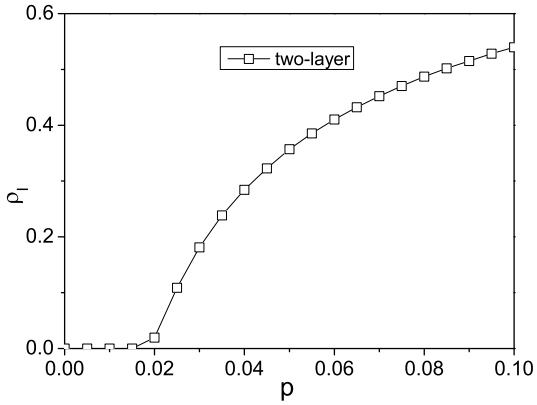

Fig. 3. ρ_I versus p on the two-layer railway-local area traveling network for $\mu = 0.1$ and $\beta = 0.008$.

network (circles). This corresponds to $\beta/\mu = 0.2$ and ρ_I is high for $p = 0.05$ from Figure 2b. Figure 2c shows that ρ_I drops gradually as p decreases until in a range of small p-values then ρ_I drops rapidly to a very small value. Thus, frequent traveling leads to a higher risk of spreading a disease. When compared with the reference ER network, the two-layer network leads to a more severe infection. When more people become travelers, the gathering of susceptible and infected travelers on the railway network has the effects of enhancing infections on the railway nodes and spreading the diseases among different local areas.

A higher p corresponds to more travelers so that they will be gathered on the railway leading to a higher ρ_I and a higher β will also lead to a higher ρ_I. Therefore, the parameters p and β may play a similar role. This can be better seen if we look at a case where $\rho_I = 0$ for $p = 0$, as for $\beta = 0.008$. Figure 3 shows that ρ_I as p increases for $\beta = 0.008$. The results show that there is a threshold $p_c \approx 0.02$ such that for $p > p_c$, ρ_I becomes finite. This phenomenon is only found in two-layered networks. With an increasing p, more people become travelers and the number of people in the railway nodes increases, making it easier for an epidemic outbreak.

3 Simplified two-layer railway-local area traveling network

The entire railway network in a country or a continent typically consists of a few major railways intersecting at some major cities. It is, therefore, also important to study the effects of a single major railway serving a number of local areas, via a simplified version of the two-layer traveling network constructed as follows. Let m local area subnetworks be constructed in the same way as above, with the node of the highest degree in each subnetwork becoming the major train station of the local area. These m major train stations are then connected in a sequence by a single major railway, as depicted schematically in Figure 4.

We consider systems consisting of $m = 10$ local-area subnetworks. Each local subnetwork i consists of $M_i = 100$ nodes (towns) forming an ER network of mean degree $\langle k \rangle = 10$, thus there are a total of $M = \sum_{i=1}^{m} = 1000$

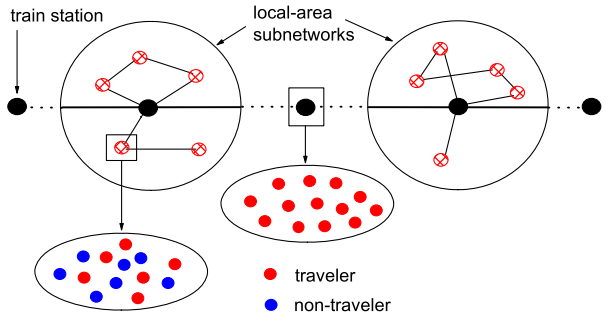

Fig. 4. (Color online) Schematic diagram showing the simplified railway-local area network model consisting of a single major railway stopping at main stations, each supported by a local-area subnetwork (big circules) serving smaller cities and towns (nodes inside big circles). There are travelers and non-travelers in the towns, while there are only travelers at the railway stations.

nodes. Keeping the same average number of persons $N/M = 10$ per node, there are altogether $N = 10^4$ individuals. The probability for a non-traveler to start a journey is $p = 0.05$, unless specified otherwise. The recovery probability in the SIS model is $\mu = 0.1$. The infection process is initialized by randomly choosing 1% of the people as infected.

Figure 5a shows how ρ_I varies with time (solid line), for an infection probability $\beta = 0.02$. Results are compared to that of an ER reference network with the same total number of nodes and mean degree (dashed line). The results are similar to those in Figure 2a. The presence of the major railway leads to a more rapid increase at short time and a more severe epidemic as given by the higher steady-state value of ρ_I. For m subnetworks of equal size, a traveler has a chance of $1-1/m$ (which is 90% for $m = 10$) to go to a destination in a different subnetwork and therefore will travel on the railway. Most travelers, infected and susceptible, will meet on the railway. This enhances the infection process on the railway and also brings more infected persons to the destinations for further infections.

Figure 5b shows the results for a higher infection probability of $\beta = 0.06$. While the increase in ρ_I is still faster in the railway-local area network than in the ER reference network, the steady-state values are almost the same for the two networks. In this case, infection is effective in the local-area nodes and on the railway, and a large portion of the population is infected. The larger value of β implies that no gathering of infected and susceptible travelers is needed for the infection to be enhanced. Similar calculations are carried out for different values of β. The results of the steady-state ρ_I are shown as a function of β/μ in Figure 5c for both the railway-local area and the ER reference networks. We see that there exists a finite ρ_I for a smaller value of β/μ in the presence of the major railway. This is similar to what we have observed in Figure 2. Thus, the enhanced epidemics in the two-layer railway-local area traveling network is due to the enhanced epidemics of each major railway.

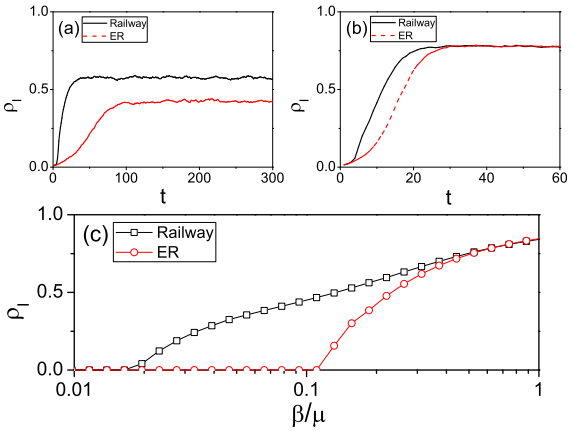

Fig. 5. (Color online) ρ_I as a function of time t for (a) $\beta = 0.02$ and (b) $\beta = 0.06$. The darker (black) lines give the results of the railway-local-area network model, and the lighter (red) lines give the results of an ER random network containing the same total number of nodes and mean degree. (c) ρ_I as a function of β/μ, for the railway-local-area network model (squares) and ER random network (circles).

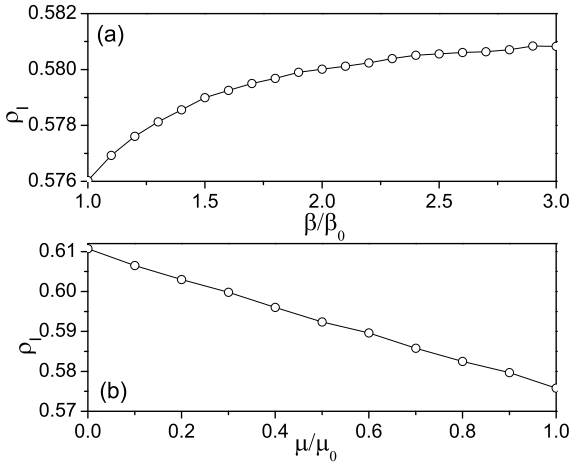

Fig. 6. Effects of enhancing the infection probability β and reducing the recovery probability μ at the main railway stations in a system with $N = 10^4$ persons. (a) ρ_I as a function of β/β_0 with $\beta_0 = 0.02$ and $\mu = \mu_0 = 0.1$. (b) ρ_I as a function of μ/μ_0 with $\mu_0 = 0.1$ and $\beta = \beta_0 = 0.02$.

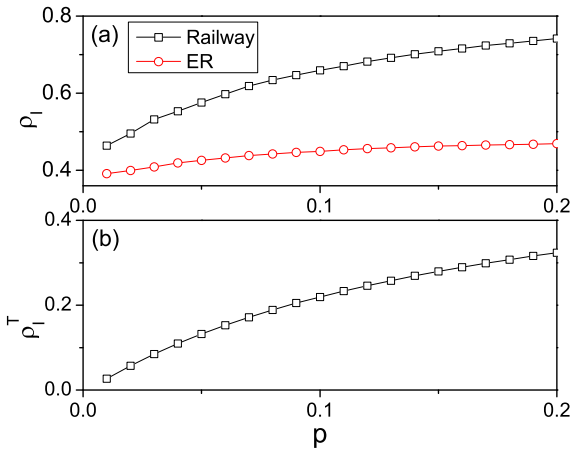

Fig. 7. (Color online) Effects of the traveling probability p on epidemics. (a) ρ_I as a function of p for both the railway-local area network (squares) and the corresponding ER network (circles); (b) ρ_I^T as a function of p.

The railway poses an additional risk factor. By gathering more people on to the nodes that the major railway serves, there is the risk of an enhanced infection probability β at these nodes, e.g., due to the closer separation between people, on top of the enhanced infection through the larger $n_{i,I}$. This can be modeled by imposing a larger value of β at the railway stations as compared to a smaller value β_0 at the other local-area nodes. This does not alter the movement and the grouping of people in the nodes. Figure 6a shows that ρ_I only increases slightly with an enhanced infection probability $\beta/\beta_0 > 1$, with $\beta_0 = 0.02$. To complete the study, Figure 6b shows the results for a reduced recovery probability $\mu/\mu_0 < 1$ in the railway stations, where $\mu_0 = 0.1$ is the recovery probability at the local-area nodes. Similar to an increased β, a suppressed μ also increases ρ_I.

We also studied the effects of the traveling probability p. Figure 7a shows the steady state value of ρ_I for different values of p in the railway-local-area network (squares) and the corresponding ER network (circles). While ρ_I increases with p in both cases, the increase is much pronounced in the railway-local-area network. With more travelers crowding the railway, the level of infection in the population becomes significantly higher. When more people become travelers, the gathering of susceptible and infected travelers on the railway has the effect of enhancing the fraction of infected agents on the railway. Let ρ_I^T be the ratio of the number of infected agents in the steady state on the railway to N. Figure 7b displays how ρ_I^T increases with p. Combining with Figure 7a, we note that while both ρ_I and ρ_I^T increase gradually with p, the ratio ρ_I^T/ρ_I increases much rapidly with p, indicating the risk that a railway poses in spreading a disease when people travel frequently.

Railways are an essential infrastructure for countries seeking economic growth, but they unavoidably gather people and pose serious risk of an epidemic. In recent years, we see major initiatives for high speed trains in different countries, for the reason of controlling carbon emissions among others. China's network of high-speed trains run at a top speed of 220 mph ($\sim$354 km h^{-1}). In the USA, there is a plan to build a $500-billion 220 mph railway network linking 80% of Americans by 2030 [1]. In Japan, a $64-billion line connecting Tokyo and Nagoya that runs at 310 mph ($\sim$500 km h^{-1}) will complete by 2045, cutting the traveling time by 58%. These high speed trains run faster, stop at fewer main stations, and are supported by bigger local-area networks serving more smaller cities and towns. To study how these features alter the extent of an infection, we present results of ρ_I^T and ρ_I for two modified systems with a reduced number of $m = 5$ and $m = 2$ main stations in Figure 8. Here, the population size ($N = 10^4$ agents), the total number of nodes ($M = 10^3$), and

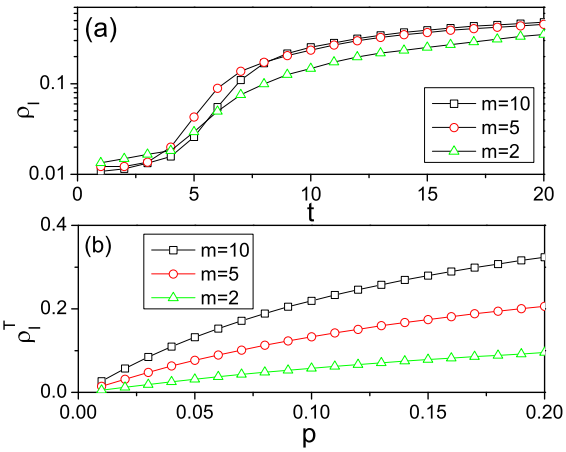

Fig. 8. (Color online) Effects of enhanced train speeds as represented by a reduced value of m. (a) $\rho_I(t)$ for $m = 2$, 5, 10 at short time. (b) ρ_I^T as a function of p for systems with $m = 10$, $m = 5$, and $m = 2$ main railway stations, representing higher speeds of the train.

the average degree ($\langle k\rangle = 10$) are retained. Therefore, the 5 (2) subnetworks for $m = 5$ ($m = 2$) each serves a local area with 200 (500) nodes. The higher speed is reflected in the single time step for traveling between main stations. In particular, Figure 8a shows that in the beginning few time steps, ρ_I is higher for $m = 2$ than $m = 5$ and 10; but after that, ρ_I becomes lower for $m = 2$. Figure 8b indicates that the drop in ρ_I^T (infected agents on the railway) is more pronounced as the speed increases, and thus the portion of infected agents on the railway drops significantly, when compared with the $m = 10$ case.

4 A theoretical model

It is possible to capture the key features observed in simulation results analytically by considering a theoretical model that ignores the randomness in the local area networks. To illustrate the idea, we focus on the SIS model with a single major railway. Figure 9 shows schematically the model based on which we develop our analytic approach. There are again m railway stations, forming a loop and thus corresponding to the period boundary condition. For simplicity, each local area network takes on a star-like network with k_{loc} nodes connecting directly to the railway station. Thus, it only takes one step for travelers to go from the local nodes to the railway station in the local area. Every railway station has a degree of $(k_{loc} + 2)$ and every local area node has a degree of unity. Numerically, we have checked that this model gives qualitatively the same behavior as in the railway-local area network model with a major railway.

To proceed, we treat the two dynamical processes separately. One process deals with how individual travels. We aim to getting at the number of travelers at the railway stations and the number of individuals in the local nodes in the steady state. With m railway stations, there are a total of mk_{loc} nodes in all the local area networks. Let N^T be the number of travelers in the railway stations or on the train, and N^{loc} be the number of individuals in all the local nodes. Thus, the number of travelers per railway station is $n^T = N^T/m$, and the number of individuals per local area node is given by $n^{loc} = N^{loc}/mk_{loc}$. Note that $N = N^T + N^{loc} = mn^T + mk_{loc}n^{loc}$ is a constant.

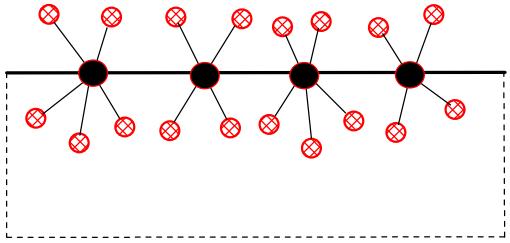

Fig. 9. (Color online) Schematic diagram showing star-like local-area networks connected to major railway stations (black dots). This model facilitates our analytic approach.

The quantities n^T and n^{loc} are coupled through the arrival of travelers at local destinations and the probability p of starting a new journal. The dynamical equations of n^T and n^{loc} are

$$\frac{dn^{loc}}{dt} = -pn^{loc} + \frac{\eta}{k_{loc}}n^T,$$
$$\frac{dn^T}{dt} = -\eta n^T + pk_{loc}n^{loc}, \quad (1)$$

where η is the probability of an individual arriving at his destination at a local area node. In the steady state, we thus have

$$n^T = \frac{pN}{m(p+\eta)},$$
$$n^{loc} = \frac{\eta N}{mk_{loc}(p+\eta)} = \frac{\eta}{pk_{loc}}n^T. \quad (2)$$

An estimation of the parameter η can be found as follows. A person will at most travel $m/2$ railway stations towards his destination. The average number of railway stations for a journey is roughly $m/4$. Thus, an individual would have a probability $\eta = 4/m \sim 1/m$ (for $m \gg 1$) to get off the railway station. Therefore, a balance between travelers arriving at their destinations and starting new journeys maintains a stable n^T and n^{loc}.

To couple the travelers' dynamics with SIS epidemics, we split n_{loc} and n_T into contributions from the susceptible and infected individuals, i.e. $n^{loc} = n_S^{loc} + n_I^{loc}$ and $n^T = n_S^T + n_I^T$ with the subscript characterizing the state. Following the SIS dynamics, we have

$$\frac{dn_I^{loc}}{dt} = (1-p)\left[(1-\mu)n_I^{loc} + \beta n_S^{loc}n_I^{loc}\right] + \frac{\eta}{k_{loc}}\left[(1-\mu)n_I^T + \beta n_S^T n_I^T\right] - n_I^{(loc)},$$
$$\frac{dn_I^T}{dt} = pk_{loc}\left[(1-\mu)n_I^{loc} + \beta n_S^{loc}n_I^{loc}\right] + (1-\eta)\left[(1-\mu)n_I^T + \beta n_S^T n_I^T\right] - n_I^T. \quad (3)$$

The total number of infected individuals is given by $N_I = mn_I^T + mk_{loc}n_I^{loc}$. It follows that

$$\frac{dN_I}{dt} = m\beta\left(k_{loc}n_S^{loc}n_I^{loc} + n_S^T n_I^T\right) - \mu N_I. \quad (4)$$

In the steady state, N_I, n_I^{loc} and n_I^T are related through

$$N_I = \frac{m\beta}{\mu}\left[k_{loc}\left(n^{loc} - n_I^{loc}\right)n_I^{loc} + \left(n^T - n_I^T\right)n_I^T\right], \quad (5)$$

where n^T and n^{loc} are given by equation (2). As $\rho_I = N_I/N$, it follows that ρ_I would increase with β/μ, as the numerical results in Figure 5c show. Note that n_I^{loc} and n_I^T will also depend on β/μ making the dependence of ρ_I on β/μ nonlinear.

For different infection probabilities β and β_0 in the railway and local-area networks, equations (3)–(5) can be modified readily. The term $\beta n_S^{loc}n_I^{loc}$ in equation (3) becomes $\beta_0 n_S^{loc}n_I^{loc}$, resulting in

$$N_I = \frac{m\beta_0}{\mu}\left(k_{loc}n_S^{loc}n_I^{loc} + \frac{\beta}{\beta_0}n_S^T n_I^T\right). \quad (6)$$

It follows that N_I would increase with β/β_0, as observed in Figure 6a. The result also indicates that the increase is significant only when there are many people on the railway, i.e. when $n_S^T n_I^T$ is large. Similarly, one can generalize to the case of different recovery probabilities.

Equation (4) can be used to explore the transient behavior. When the infection begins, we have $n_I^{loc} \ll n_S^{loc}$ and $n_I^T \ll n_S^T$. One can then linearize equation (4) to give

$$\begin{aligned}\frac{dN_I}{dt} &\approx m\beta\left(k_{loc}n^{loc}n_I^{loc} + n^T n_I^T\right) - \mu N_I \\ &= \beta\left(N^{loc}n_I^{loc} + N^T n_I^T\right) - \mu N_I, \end{aligned} \quad (7)$$

where the terms $(n_I^{loc})^2$ and $(n_I^T)^2$ are ignored. Since $n_I^{loc} = (N_I - mn_I^T)/mk_{loc}$, we have

$$\begin{aligned}\frac{dN_I}{dt} &= \beta\left(n^{loc}N_I + \left(n^T - n^{loc}\right)mn_I^T\right) - \mu N_I \\ &\approx \beta\left(n^{loc}(1-\chi) + n^T\chi\right)N_I - \mu N_I, \end{aligned} \quad (8)$$

where $\chi \equiv N_I^T/N_I$ represents the ratio of infected number in the stations to the total infected number in the system and $0 < \chi < 1$. Solving equation (8) for $N_I(t)$ and thus $\rho_I(t)$ at short times gives

$$\rho_I(t) = \rho_I(0)e^{\left[\beta\left(n^T\chi + n^{loc}(1-\chi)\right) - \mu\right]t}. \quad (9)$$

This result is consistent with numerical results. The initial exponential growth shows that the gathering of agents, including infected ones, at the major railway stations as given by the factor $(n^T\chi)$ leads to a faster initial growth in $\rho_I(t)$ than in ER network. In contrast, $\rho_I(t) \sim e^{(\beta n - \mu)t}$ in an ER network, where $n = N/M$ is the average number of persons per node in the absence of the major railway, shows a slower initial growth. This is consistent with simulation results shown in Figures 5a and 5b. In addition, a smaller value of m would lead to a higher n^T and thus a faster initial growth and thus a higher ρ_I at short times, as seen in Figure 8a. Equation (9) also shows that gathering of travelers on the railway leads to a smaller infection threshold, as $\beta/\mu > 1/(n^T\chi + n^{loc}(1-\chi)) = 1/[(n^T - n^{loc})\chi + n^{loc}]$ would lead to an initial growth in ρ_I. In contrast, the corresponding ER network gives a threshold $\beta/\mu > 1/n$. Considering that n^T is generally much larger than n^{loc} and $n^{loc} \approx n$, we conclude that $1/[(n^T - n^{loc})\chi + n^{loc}] < 1/n$, indicating that the threshold $(\beta/\mu)_c$ for the two-layered network will be less than that of the corresponding ER network. This is consistent with the numerical results in Figure 5c.

5 Summary

In summary, we presented and studied two-layer traveling network models that capture several essential features of modern high speed train systems and studied a coevolving epidemic with individuals traveling on the networks. A railway network and the role of a single major railway were studied in the SIS model. A major railway, which gathers traveling individuals, would lead to a faster initial infection and a more severe level of infection in the steady state, when compared with a random ER network consisting of all the nodes. Higher speed trains, which stop at fewer stations each serving a bigger local area, help suppress the level of infection. An analytic treatment, based on a model that emphasizes the role of the major railway, reveals the key features observed in simulation results. The results represent a step towards a better design of control strategies in modern transportation systems. We remark that we have also carried out similar studies using the SIR model, where R denotes the recovered persons. The many effects that we discussed with regard to the SIS model also apply to the SIR model. We remark that while the present model and analysis included a number of new features, a more realistic study incorporating real data on the local transportation design, multiple major railways, and distribution of population would require much more work than here.

The present work can be extended to other types of two-layer transportation networks, including the coupling of airports, subways, coaches and local buses. It can also be extended to individuals moving in a multi-layered network. Another key feature into the models is that the travelers take on the shortest path towards the destination, instead of the random diffusion processes studied in previous works. This highly directional or driven process can be extended to other problems such as heat and mass transportation in multi-layered networks. These problems are worthy of further investigations.

This work was supported in part by the NNSF of China under Grant Nos. 10975053 and 11135001 (Z.L.), and the Research Grants Council of Hong Kong SAR Government under Grant No. CUHK-401109 (P.M.H). Z. Liu would like to thank the Chinese University of Hong Kong for the hospitality during a visit when part of the work was carried out.

References

1. See the website of the US High Speed Rail Association at http://www.ushsr.com/ushsrmap.html for a plan of high speed trains linking 80% of Americans by 2030. The plan of a 310 mph line in Japan was reported in New York Times in February 2011, see http://intransit.blogs.nytimes.com/2011/02/14/japan-plans-worlds-fastest-train/
2. R. Albert, A.-L. Barabasi, Rev. Mod. Phys. **74**, 47 (2002)
3. M.E.J. Newman, Phys. Rev. E **66**, 016128 (2002)
4. M. Boguna, R. Pastor-Satorras, A. Vespignani, Phys. Rev. Lett. **90**, 028701 (2003)
5. C. Castellano, R. Pastor-Satorras, Phys. Rev. Lett. **105**, 218701 (2010)
6. Y. Schwarzkopf, A. Rakos, D. Mukamel, Phys. Rev. E **82**, 036112 (2010)
7. R. Pastor-Satorras, A. Vespignani, Phys. Rev. Lett. **86**, 3200 (2001)
8. V.M. Eguiluz, K. Klemm, Phys. Rev. Lett. **89**, 108701 (2002)
9. T. Gross, C.J. Dommar D'Lima, B. Blasius, Phys. Rev. Lett. **96**, 208701 (2006)
10. R. Parshani, S. Carmi, S. Havlin, Phys. Rev. Lett. **104**, 258701 (2010)
11. C. Moore, M.E.J. Newman, Phys. Rev. E **61**, 5678 (2002)
12. M. Kuperman, G. Abramson, Phys. Rev. Lett. **86**, 2909 (2001)
13. R. Pastor-Satorras, A. Vespignani, Phys. Rev. E **63**, 066117 (2001)
14. M. Barthelemy, A. Barrat, R. Pastor-Satorras, A. Vespignani, Phys. Rev. Lett. **92**, 178701 (2004)
15. R. Olinky, L. Stone, Phys. Rev. E **70**, 030902(R) (2004)
16. Y. Moreno, R. Pastor-Satorras, A. Vespignani, Euro. phys. J. B **26**, 521 (2002)
17. Y. Moreno, J.B. Gomez, A.F. Pacheco, Phys. Rev. E **68**, 035103(R) (2003)
18. Y. Moreno, M. Nekovee, A. Vespignani, Phys. Rev. E **69**, 055101 (2004)
19. Z. Liu, B. Hu, Europhys. Lett. **72**, 315 (2005)
20. M. Salathe, J.H. Jones, PLoS Comput. Biol. **6**, e1000736 (2010)
21. F. Peruani, G.J. Sibona, Phys. Rev. Lett. **100**, 168103 (2008)
22. V. Colizza, A. Vespignani, J. Theor. Biol. **251**, 450 (2008)
23. S. Riley, Science **316**, 1298 (2007)
24. J. Zhou, Z. Liu, Physica A **388**, 1228 (2009)
25. Z. Liu, Phys. Rev. E **81**, 016110 (2010)
26. P. Wang, M.C. Gonzalez, C.A. Hidalgo, A.-L. Barabasi, DOI: 10.1126/science.1167053 (2009)
27. M. Frasca, A. Buscarino, A. Rizzo, L. Fortune, S. Boccaletti, Phys. Rev. E **74**, 036110 (2006)
28. V. Colizza, R. Pastor-Satorras, A. Vespignani, Nature Phys. **3**, 276 (2007)
29. V. Colizza, A. Vespignani, Phys. Rev. Lett. **99**, 148701 (2007)
30. M. Tang, Z. Liu, B. Li, Europhys. Lett. **87**, 18005 (2009) and references therein
31. N.M. Ferguson, D.A.T. Cummings, C. Fraser, J.C. Cajka, P.C. Cooley, D.S. Burke, Nature **442**, 448 (2006)
32. R. Pastor-Satorras, A. Vespignani, Phys. Rev. E **65**, 036104 (2002)
33. L.K. Gallos, F. Liljeros, P. Argyrakis, A. Bunde, S. Havlin, Phys. Rev. E **75**, 045104(R) (2007)
34. C. Cauchemez, A.-J. Valleron, P.-Y. Boelle, A. Flahault, N. M. Ferguson, Nature **452**, 750 (2008)
35. H. Zhang, J. Zhang, C. Zhou, M. Small, B. Wang, New J. Phys. **12**, 023015 (2010)
36. Z. Liu, Y.-C. Lai, N. Ye, Phys. Rev. E **67**, 031911 (2003)
37. I.B. Schwartz, L.B. Shaw, Physics **3**, 17 (2010)
38. Z. Zhao, J.P. Calderon, C. Xu, G. Zhao, D. Fenn, D. Sornette, R. Crane, P.M. Hui, N.F. Johnson, Phys. Rev. E **81**, 056107 (2010)
39. M. Kurant, P. Thiran, Phys. Rev. Lett. **96**, 138701 (2006)
40. M. Kurant, P. Thiran, P. Hagmann, Phys. Rev. E **76**, 026103 (2007)
41. S.V. Buldyrev, R. Parshani, G. Paul, H.E. Stanley, S. Havlin, Nature **464**, 1025 (2010)
42. R. Parshani, S.V. Buldyrev, S. Havlin, Phys. Rev. Lett. **105**, 048701 (2010)
43. S. Zou, T. Zhou, A. Liu, X. Xu, D. He, Phys. Lett. A **374**, 4406 (2010)
44. L. Hufnagel, D. Brockmann, T. Geisel, Proc. Natl. Acad. Sci. USA **101**, 15124 (2004)
45. V. Colizza, A. Barrat, M. Barthelemy, A. Vespignani, Proc. Natl. Acad. Sci. USA **103**, 2015 (2006)
46. S. Meloni, A. Arenas, Y. Moreno, Proc. Natl. Acad. Sci. USA **106**, 16897 (2009)
47. D. Balcan, V. Colizza, B. Goncalves, H. Hu, J.J. Ramasco, A. Vespignani, Proc. Natl. Acad. Sci. USA **106**, 21484 (2009)
48. http://en.wikipedia.org/wiki/Template: Main Railway Hub Station in China.
49. H. Zhang, Z. Liu, M. Tang, P.M. Hui, Phys. Lett. A **364**, 177 (2007)
50. W.E. Balbach, N.B. Frantz, B.R. Mershman, W.T. Weger, http://academic.udayton.edu/muhammadusman/2010Stander/H1N1.pdf